Elettra Sincrotrone Trieste

# XAS studies in Environmental and Materials Sciences

Giuliana Aquilanti
giuliana.aquilanti@elettra.eu

November 18, 2014

# Table of Contents

Elettra Sincrotrone Trieste

# Table of Contents

# X-ray absorption spectroscopy - 1

XAS measures the absorption coefficient as a function of energy

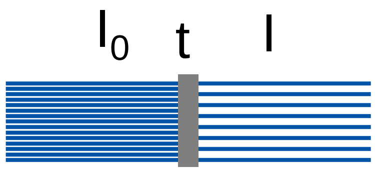


$\alpha = \mu t = \ln ( I_0 / I )$

Isolated atoms

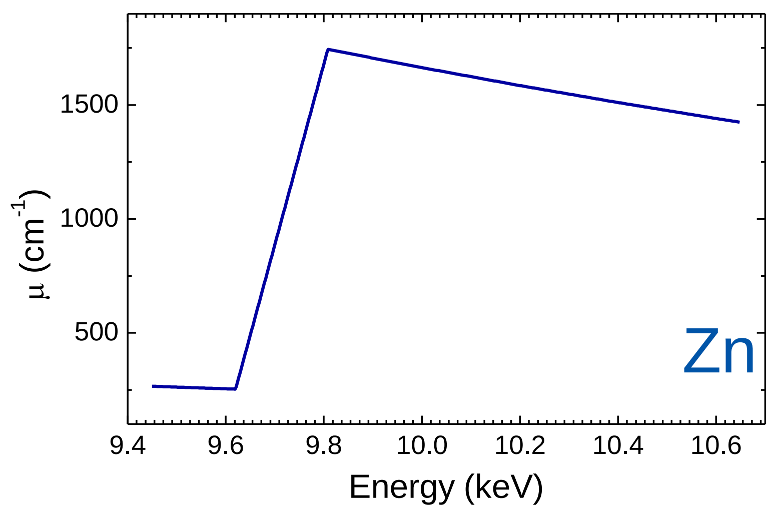


- smooth function
- sharp rise at given energies

  Signature of the element

  **chemical selectivity**

## Photoelectric effect

- An x-ray photon is absorbed by an atom when the energy of the x-ray is transferred to a core-level electron (*K*, *L*, or *M* shell) which is ejected from the atom.
- The atom is left in an *excited state* with an empty electronic level (a *core hole*).
- Any excess energy from the x-ray is given to the ejected *photoelectron*.

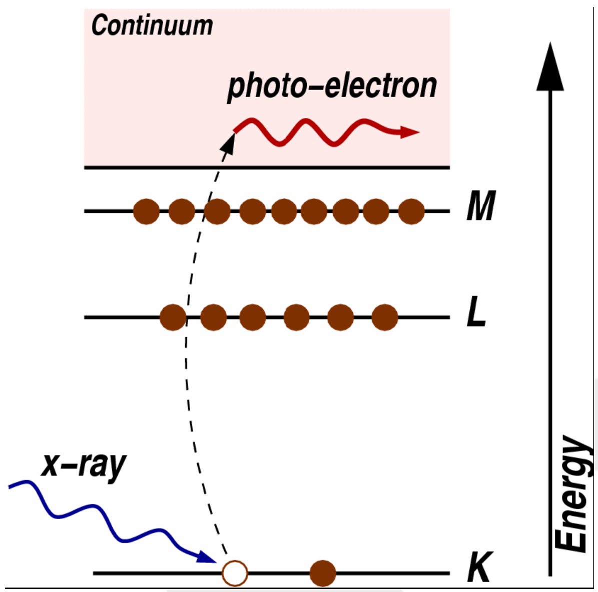

# X-ray absorption spectroscopy - 2

## Non isolated atoms

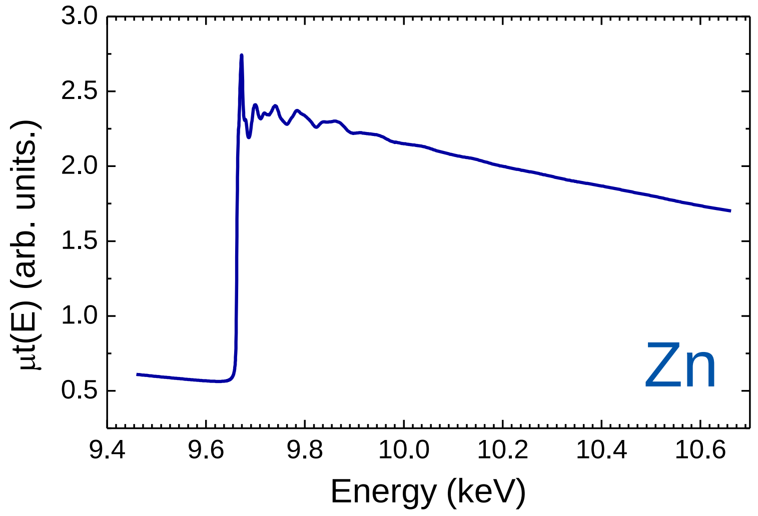


- oscillatory structures modulating the absorption
- origin:

  scattering of the photoelectron by its environment

  interference between
  the outgoing and the backscattered waves

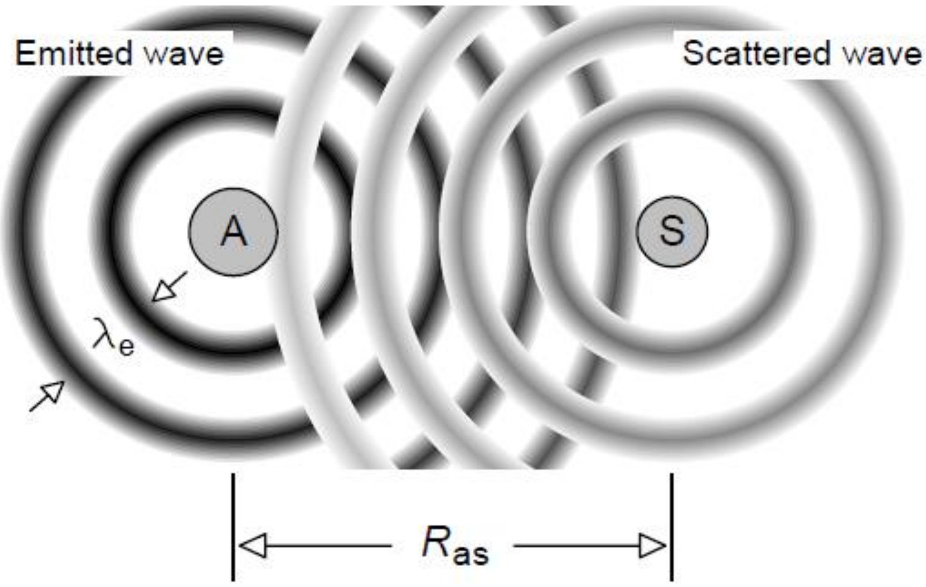


| | |
|---|---|
| Extended | X-ray |
| X-ray | Absorption |
| Absorption | Near |
| Fine | Edge |
| Structure | Structure |

# EXAFS and XANES

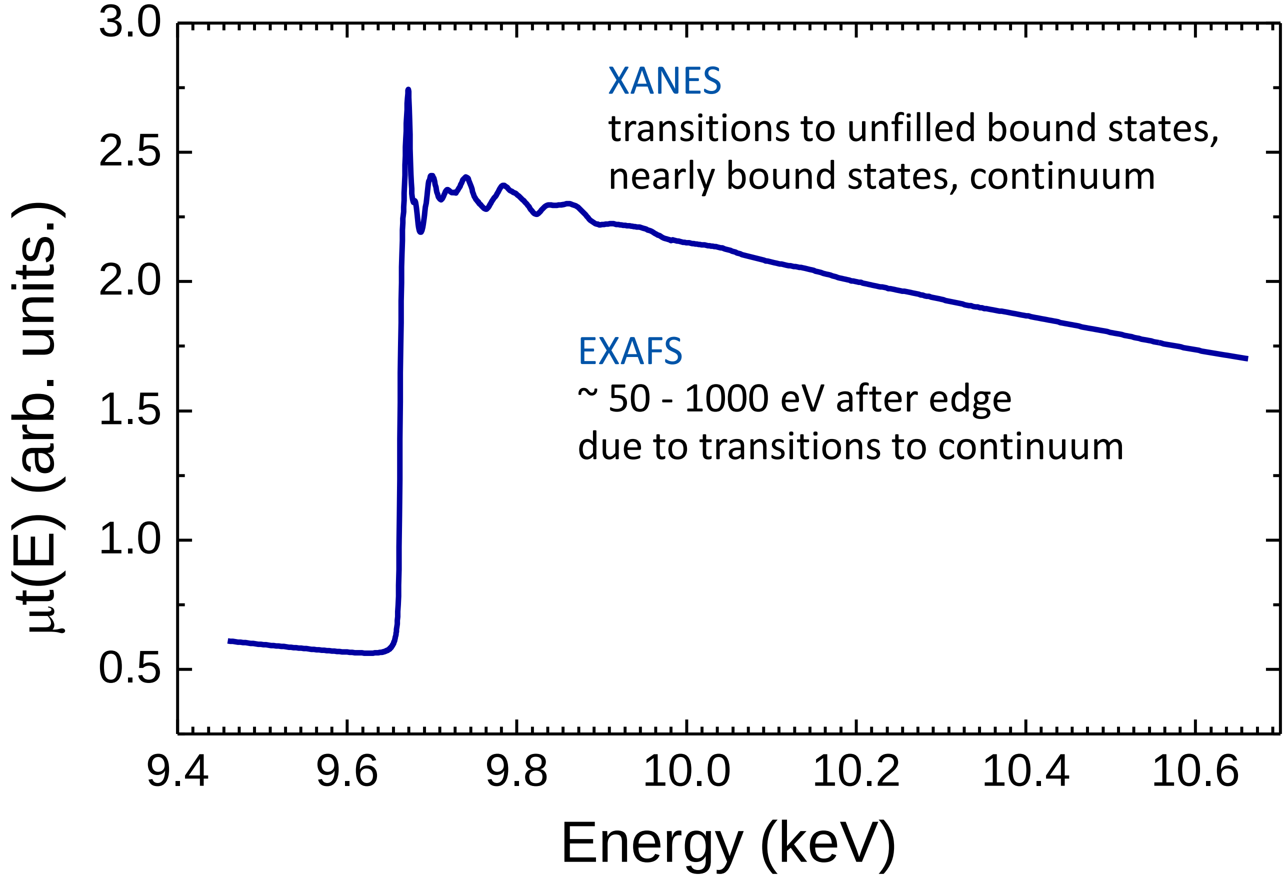


XANES: local site symmetry, charge state, orbital occupancy

EXAFS: local structure (bond distance, number, type of neighbors….)

Elettra Sincrotrone Trieste

# XAS vs. Diffraction Methods

## Diffraction Methods (X-rays, Neutrons)

- Crystalline materials with long-range ordering -> 3D picture of atomic coordinates
- Materials with only short-range order (amorphous solid, liquid, or solution) ->1D RDF containing interatomic distances due to all atomic pairs in the sample

## XAFS

- 1D radial distribution function (centered at the absorber)
- Element selectivity
- Higher sensitivity to local distortions (i.e. within the unit cell)
- Charge state sensitivity (XANES)
- Structural information on the environment of each type of atom:
    - distance, number, kind, static and thermal disorder
    - 3-body correlations
- Investigation of matter in the solid (crystalline or amorphous), liquid, solution or gaseous state with same degree of accuracy.

Elettra Sincrotrone Trieste

# Table of Contents

# The case of chromium

Pre-peaks in Cr compounds have a quadrupolar character (1s->3d bound states)

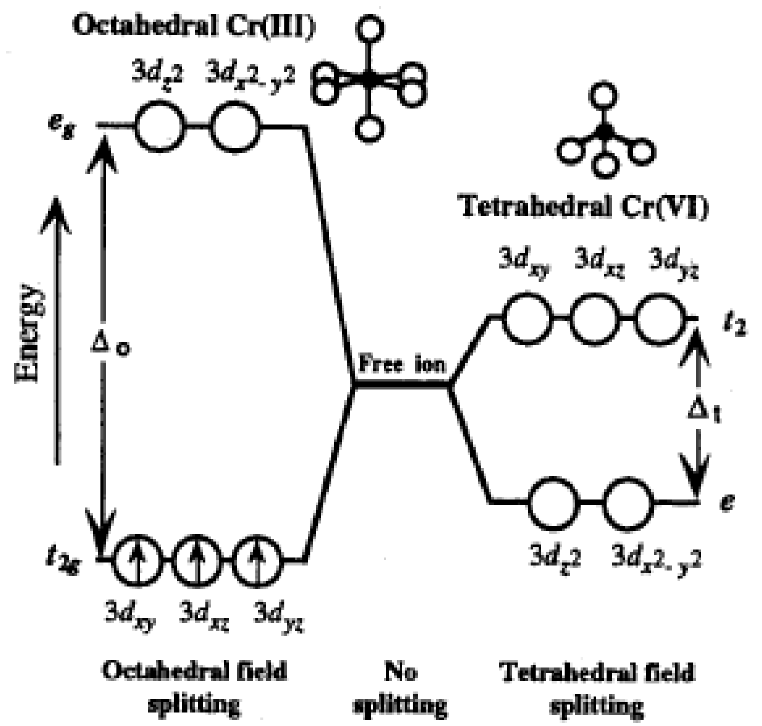


Fig. 1. Schematic illustration of octahedral crystal field splitting, $\Delta_o$, of $Cr(III)O_6$ with $d^3$ electronic configuration, and tetrahedral crystal field splitting, $\Delta_t$, of $Cr(VI)O_4$ which has an empty d orbital.

Cr(III)
- octahedral symmetry
- centrosymmetric geometry
- no p-d mixing allowed
- $d^3$ electronic configuration

Cr(VI)
- tetrahedral symmetry
- non centrosymmetric geometry
- p-d mixing allowed
- $d^0$ electronic configuration

Peterson et al., Geochimica et Cosmochimica Acta **61**, 3399 (1997)

# The case of chromium

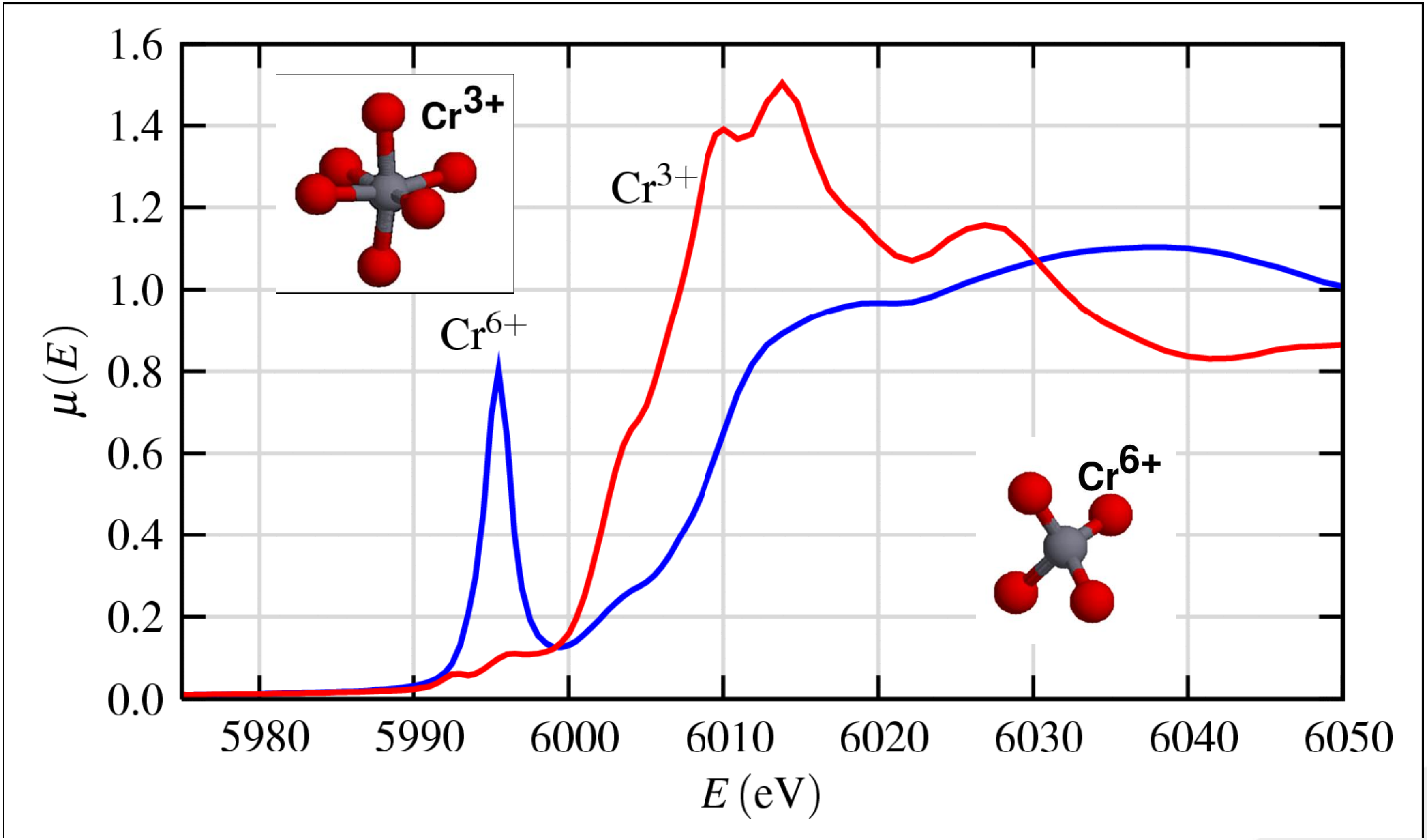

# Identification of Cr(III) and Cr(VI)

- The size of the prepeak can be used to quantify the proportion of Cr(VI) in a sample if the Cr(VI) fraction is > 5-6 % of  the total Cr.

- Prepeak calibration: peak area or height, EXAFS analysis

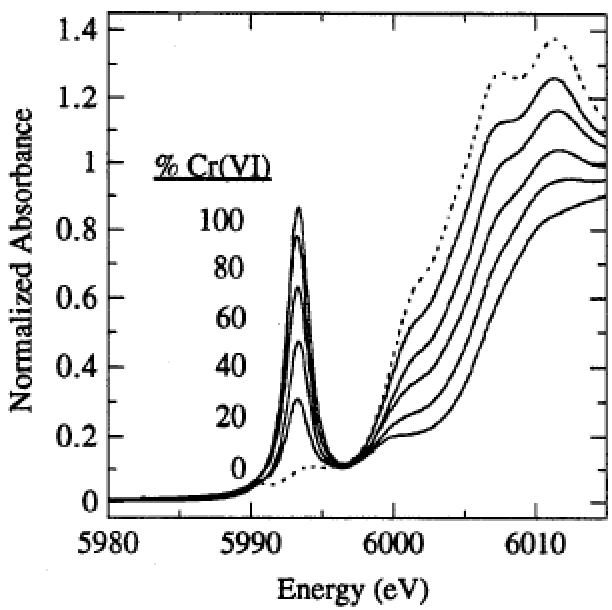


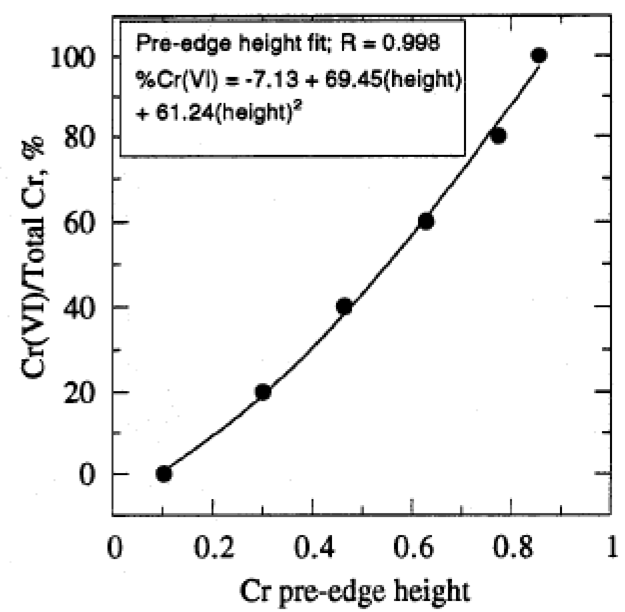


Peterson et al., Geochimica et Cosmochimica Acta **61**, 3399 (1997)

# Example: The role of magnetite in soil for Cr(VI) reduction

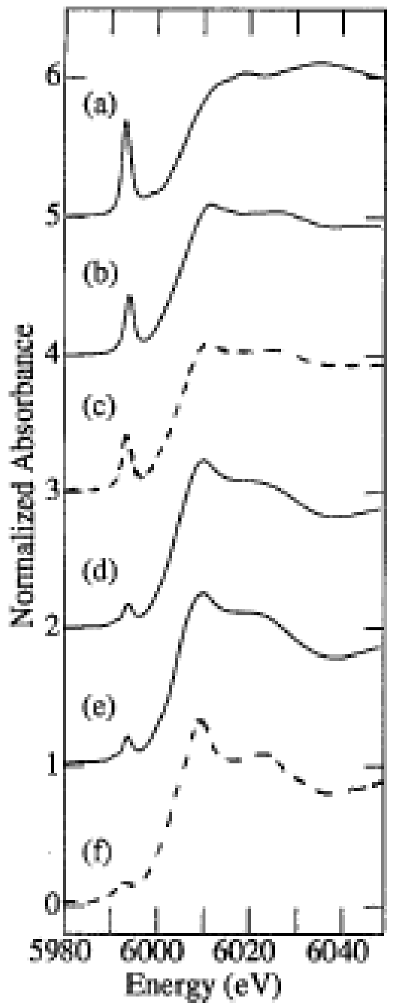


- - - Cr associated with the magnetite fraction of the soil

___ Cr not associated with the magnetite fraction of the soil

Fe(II) in magnetite may act as an electron source for heterogeneous Cr(VI)-to-Cr(III) reduction

Peterson et al., Geochimica et Cosmochimica Acta **61**, 3399 (1997)

# Example: The role of milk serum for Cr(VI) reduction

- soil near Brescia (northern Italy) contaminated by industrial activity
- Soil treated with milk serum (electron donor)

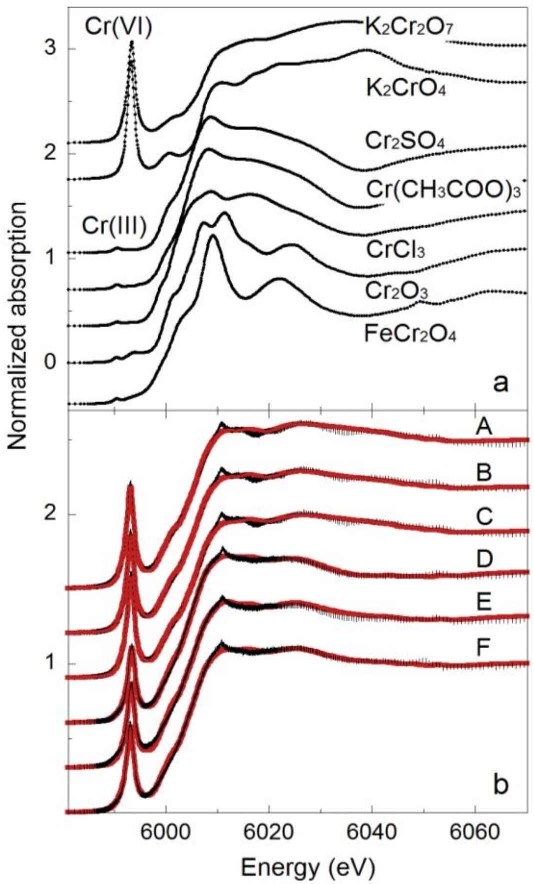


| | Cr mg/Kg | $K_2Cr_2O_7$ % | $Cr_2O_3$ % | $Cr(CH_3COO)_3$ % | Σ % | $\chi_v^2$ x$10^4$ |
|---|---|---|---|---|---|---|
| **A-nt** | 3774 | 68 | 26 | 6 | 100 | 2.5 |
| **B-nt** | 3547 | 66 | 24 | 11 | 100 | 2.1 |
| **C-nt** | 3849 | 68 | 23 | 9 | 101 | 2.3 |
| **D-t** | 3157 | 49 | 21 | 31 | 101 | 2.0 |
| **E-t** | 3449 | 53 | 27 | 21 | 101 | 3.6 |
| **F-t** | 4329 | 57 | 18 | 26 | 101 | 1.6 |

P. Lattanzi et al., Submitted

# The case of arsenic - 1

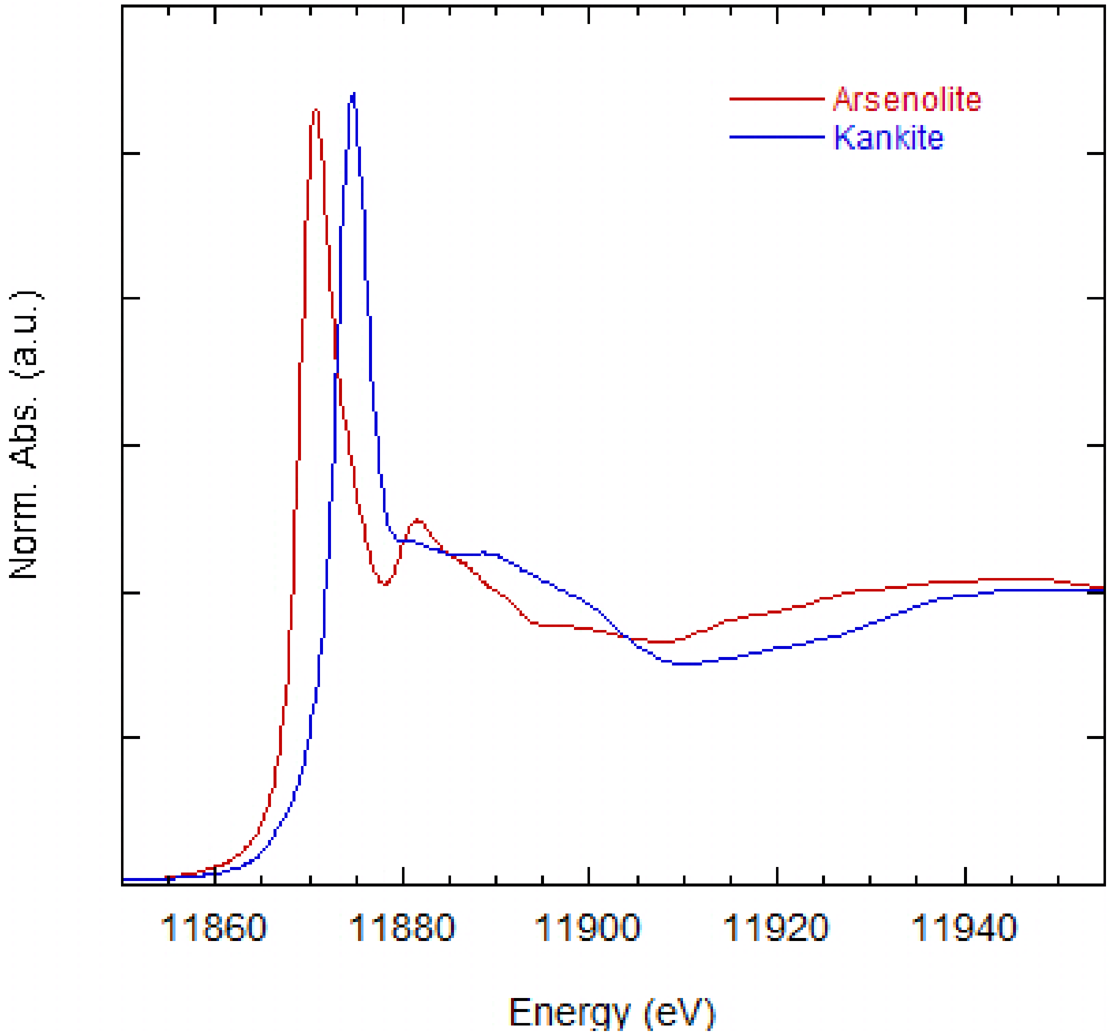


- With increasing oxidation state, the K edge is shifted to higher energies.

- For a given type of ligand, a linear relation between the edge shift and the valence state can be established

# The case of arsenic - 2

As(III)
$As_2O_3$
$E_0$=11870 eV
As-O CN 6 at 1.8 Ang

As(V)
$As_2O_5$
$E_0$=11873.5 eV
As-O CN 5 at 1.69 Ang

As(III)

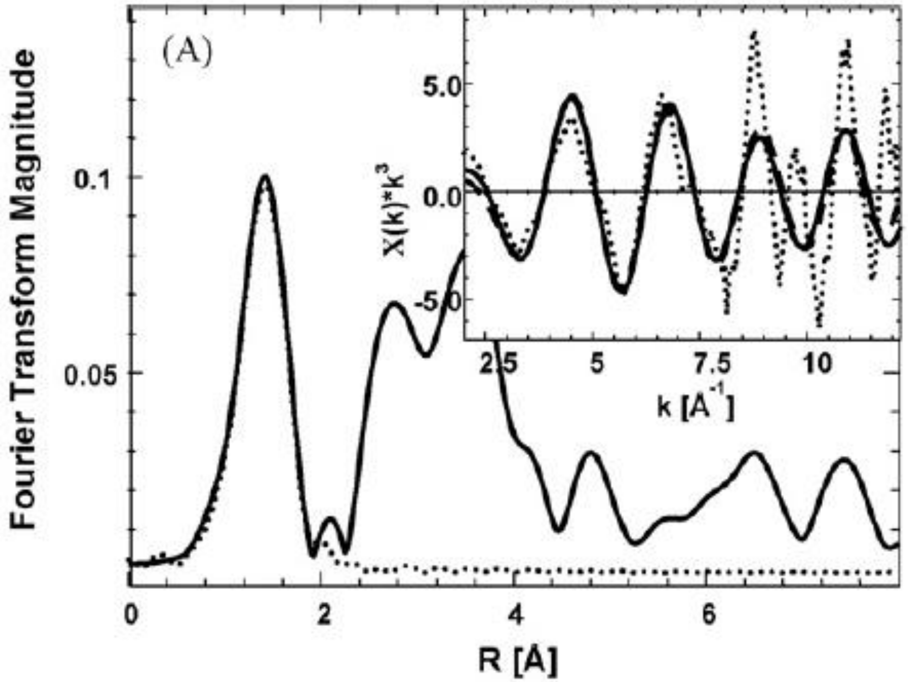


As(V)

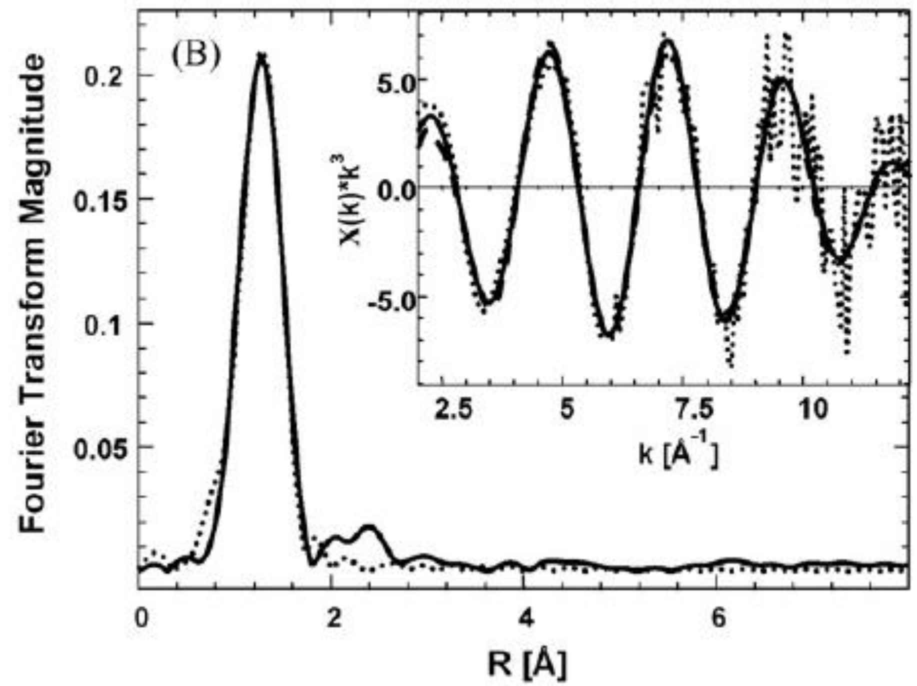

# Example: As speciation in mine site - 1

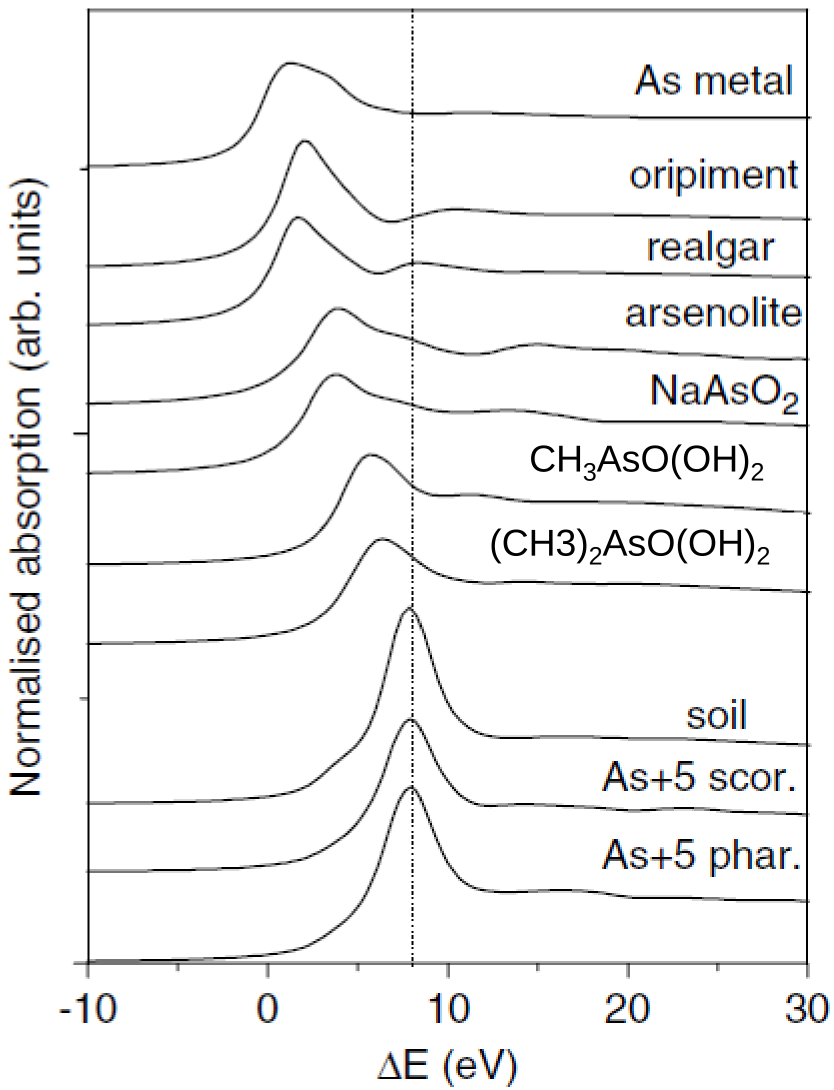


scorodite

pharmacosiderite

- The edge position in the soil sample coincides with those of the As(V) minerals.
- As in soil is predominantly in pentavalent form
- In addition, the shape of the K-edge is similar to the two As (V) minerals where As is tetrahedrally coordinated with oxygen

Arcon et al., X-ray spectrometry **34**, 453 (2005)

Elettra Sincrotrone Trieste

# Example: As speciation in mine site - 2

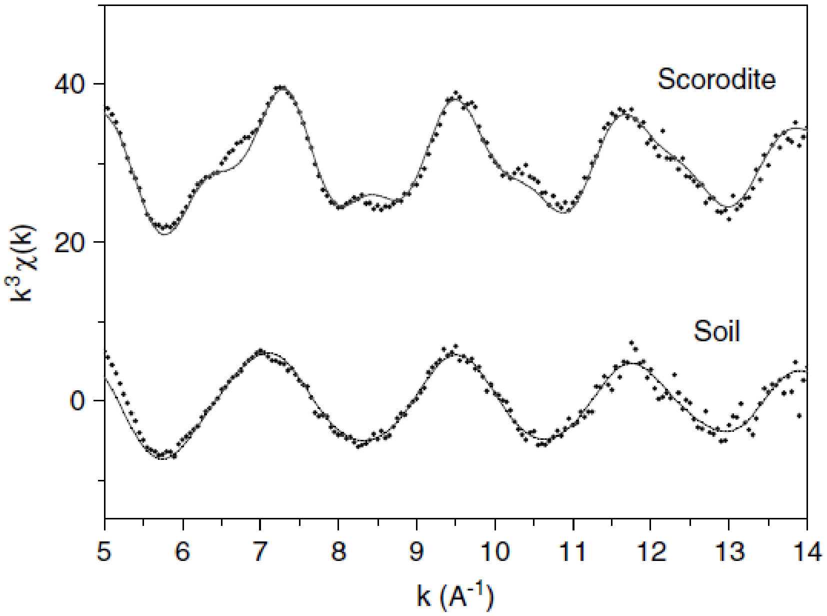


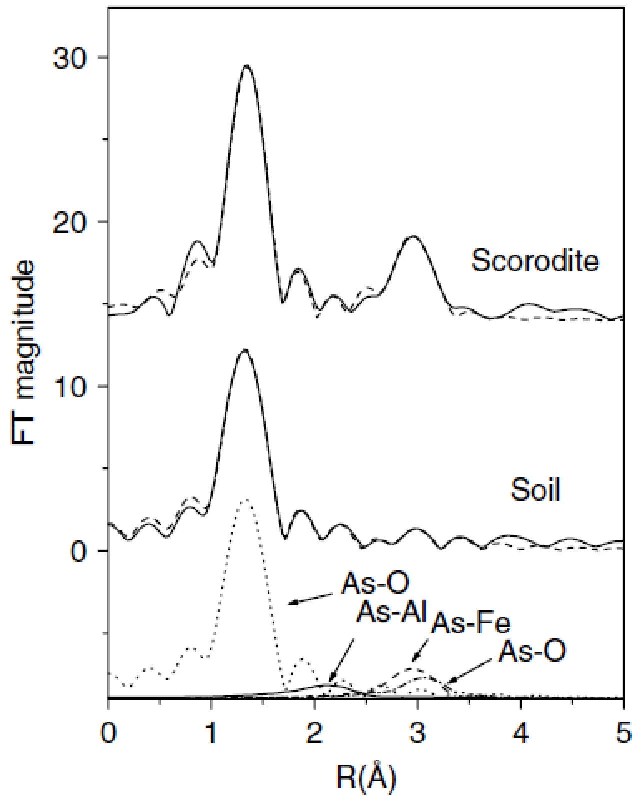


- same main frequency (same 1st coordination shell)
- second shell of scorodite absent in the soil (As in non-crystalline scorodite)

- (Non crystalline) scorodite ($FeAsO_4{\cdot}2H_2O$): principal As carrier

- Presence of Al/Si suggests that arsenate is partially adsorbed on Al (hydr)oxide or aluminosilicates (clay)

Arcon et al., X-ray spectrometry **34**, 453 (2005)

# Examples: road dust particles - 1

- Samples from *Traforo del San Bernardo* highway tunnel
- Speciation of Fe and Mn

Ideal sample area:

i) average emission from different vehicles using different fuels
ii) comes only from vehicular emission
iii)no temperature fluctuation
iv)no photo-induced effects

Bardelli et al., J. Phys.: Conf. Series **190**, 012192 (2009)

# Examples: road dust particles - 2

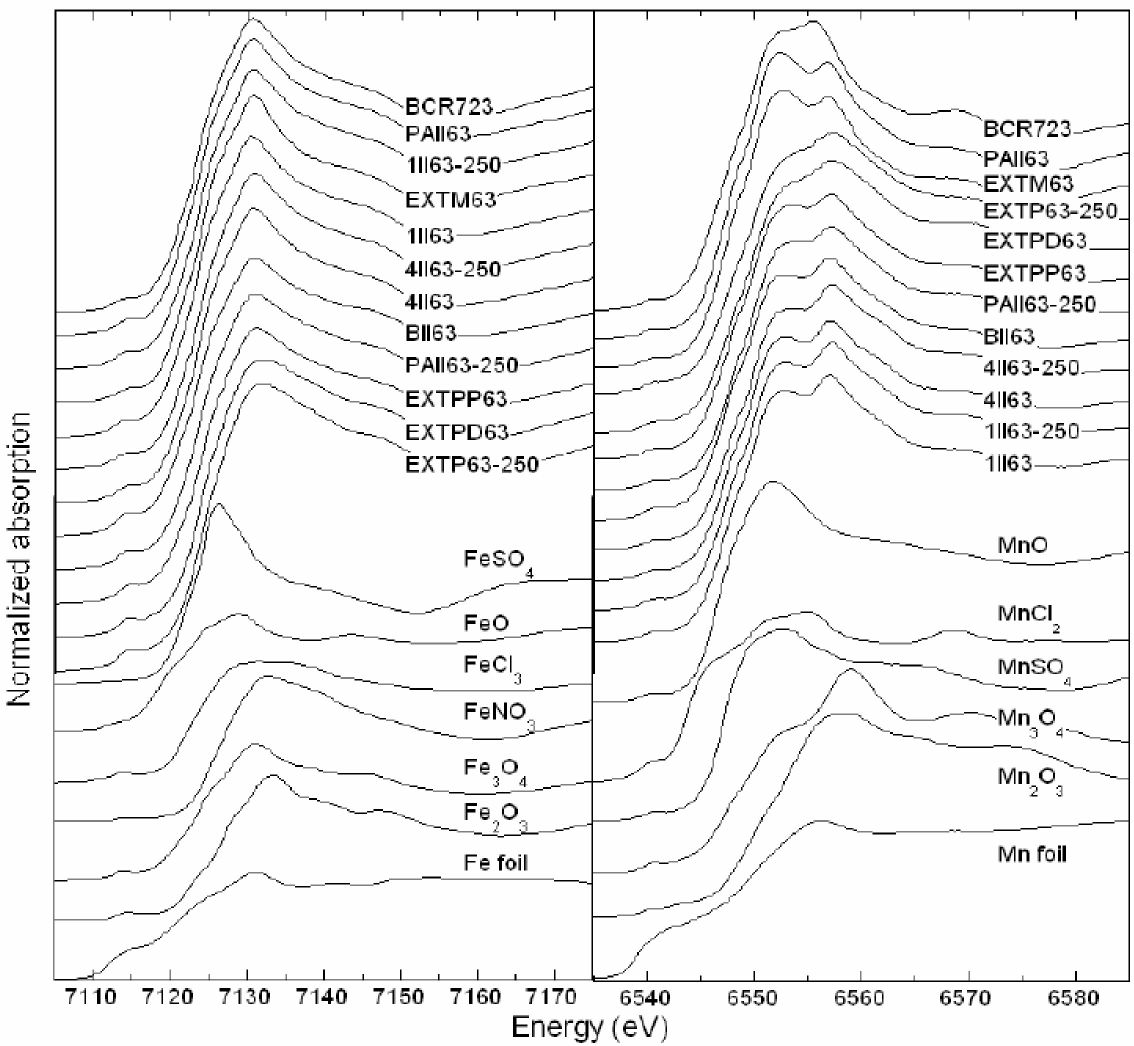


Bardelli et al., J. Phys.: Conf. Series **190**, 012192 (2009)

Data analysis method

PCA
(principal component analysis)
+
LCF
(linear combination fitting)

## PCA

- Determination of the minimum number of components necessary to reconstruct the experimental spectrum
- Identification of the best candidates

## LCF

- Estimation of the relative concentration of the candidates selected by PCA

# Table of Contents

- XAS: basic concepts
- Applications to Environmental sciences
- Applications to Materials Sciences

Elettra Sincrotrone Trieste

# General paradigma

A close relationship exists between the structure (long and short range) and the function of a material

⬇

To know the structure and to relate it to the properties of a given functional material means to be able to tailor the characteristics of the material for a targeted task

# Multiferroics: $BiFeO_3$

- Simulteneous electric and magnetic order
- Ferroelectricity and ferromagnetism require two opposite mechanisms:
  - $d^0$ configuration (FE)
  - $d^n$ configuration (FM)
- Bismuth ferrite ceramic: 'holy grail' as it is magnetic and ferroelectric at RT ($T_C$ ~ 1103 K, $T_N$ ~ 643 K)
- Potential applications: magneto-electric random access memory
- Doping improves the magnetic behaviour

# Undoped $BiFeO_3$ as a f(T)

## Study across the magnetic transition at the Fe K-edge


- All the parameters show an anomaly at $T_N$,
The magnetic transition is associated to a local structural modification around Fe

- With increasing temperature
the Fe-O distribution becomes more gaussian,
well before the ferroelectric transition

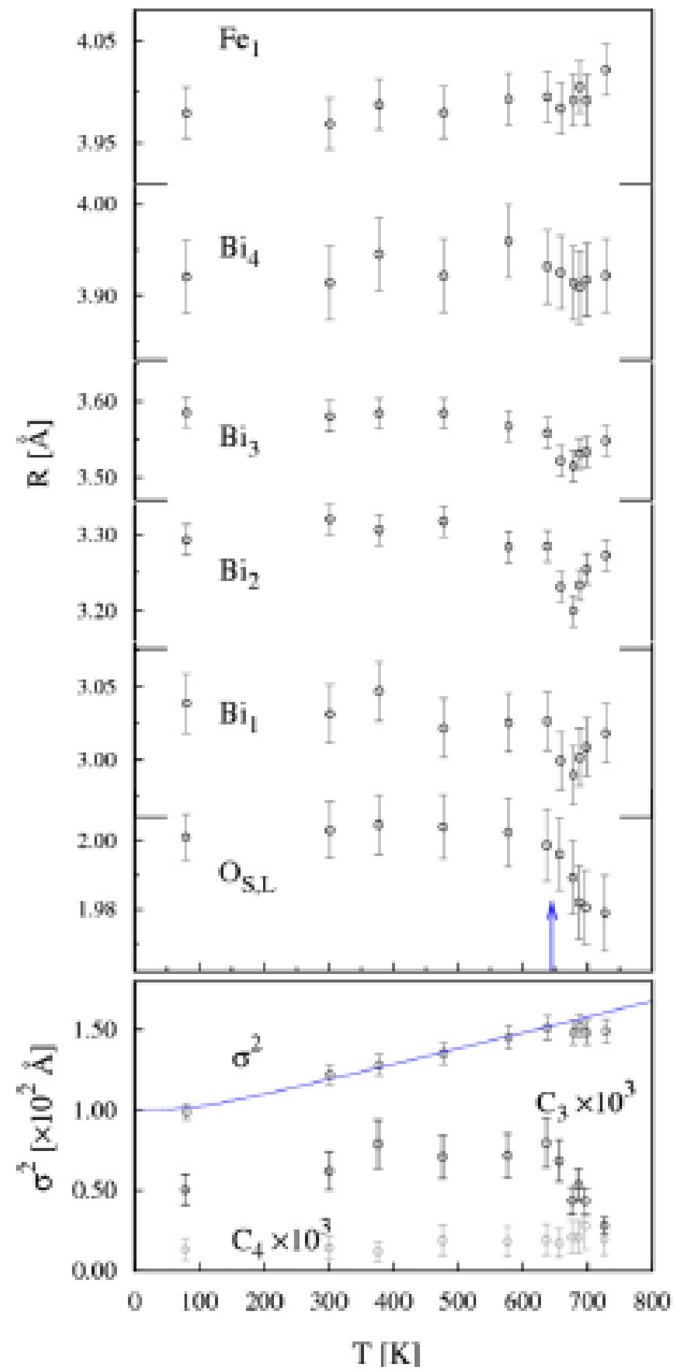


V. R. Reddy et al., JPCM **24**, 336005 (2012)

# $Eu^{3+}$ doped $BiFeO_3$ with varying $Eu^{3+}$ content

Combined XRD, Mossbauer, XAFS study

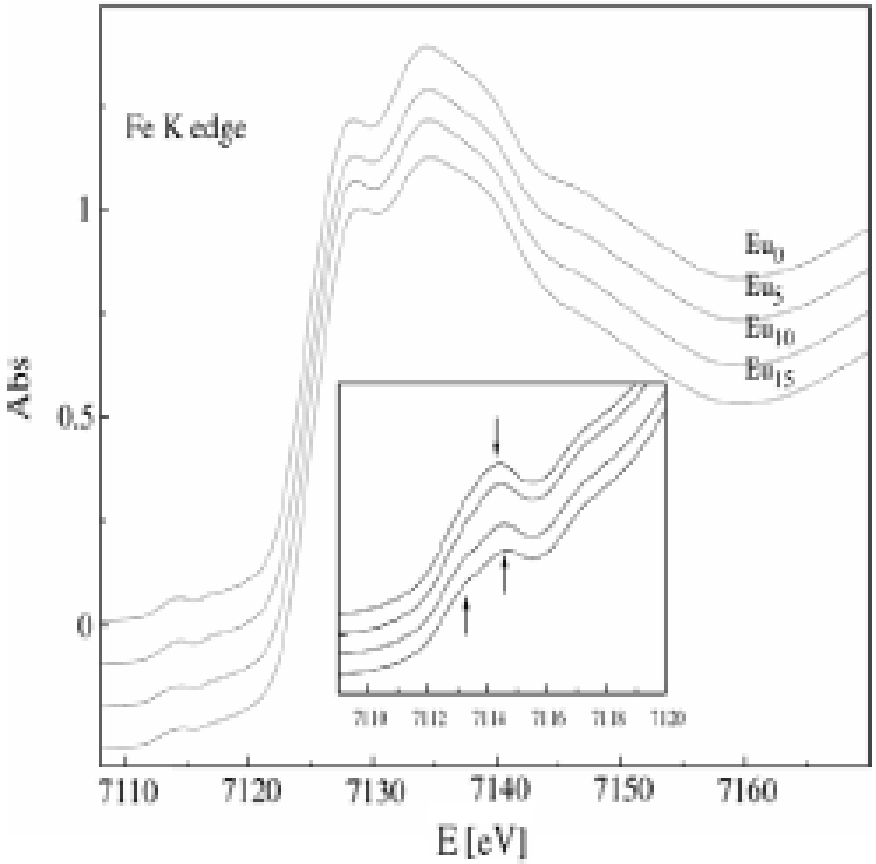


- XANES unchanged with increasing Eu doping
- Pre-edge splitting
  - Separation of the $t_{2g}$ and $e_{2g}$
  - Symmetrization of the Fe-O distribution

The improvement of the magnetic properties is due to a structural deformation

D. Kothari et al., JPCM **22**, 356001 (2010)

# Nanomaterials: identification

FeCo alloy NPs embedded on mesoporous silica

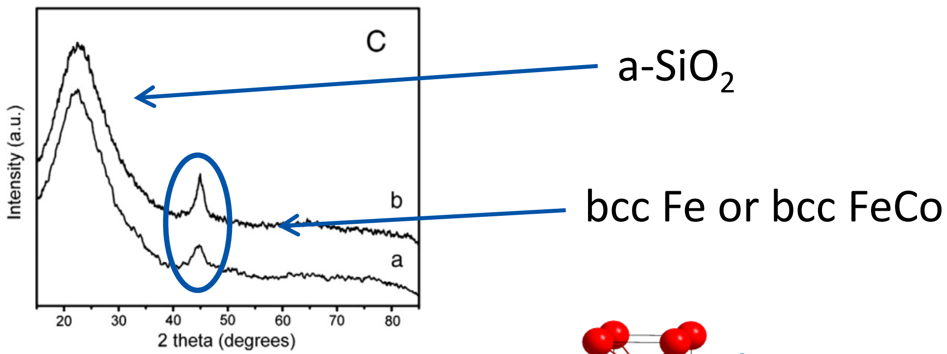


Two prep methods:

a) co-precipitation
b) impregnation

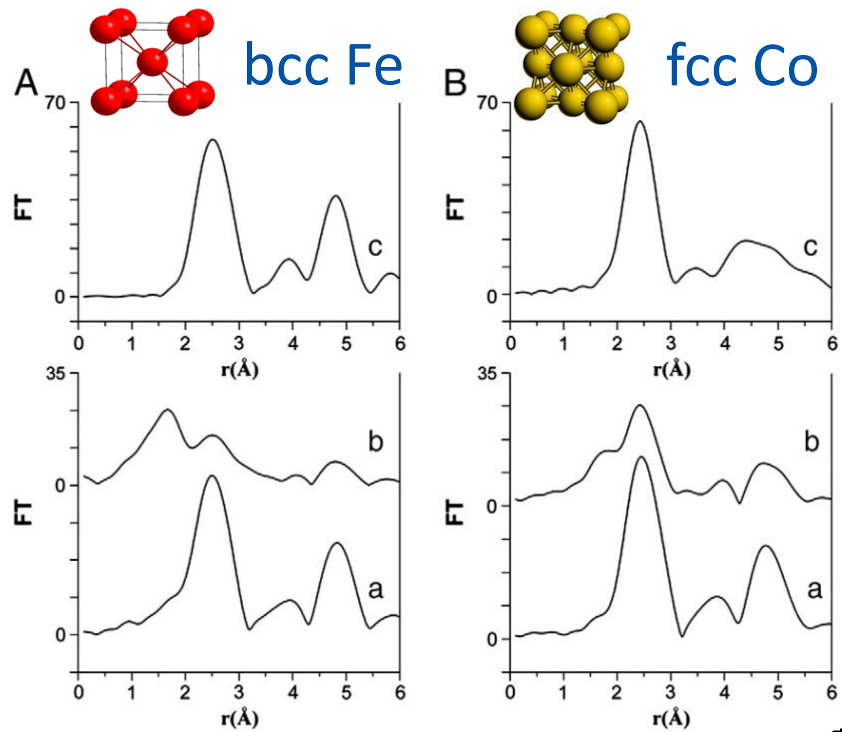


Carta et al.,
J. of Non-Cryst. Sol. **357** 2611 (2011)

# Nanomaterials: identification and characterization

## Gold NPs supported on commercial silica beads

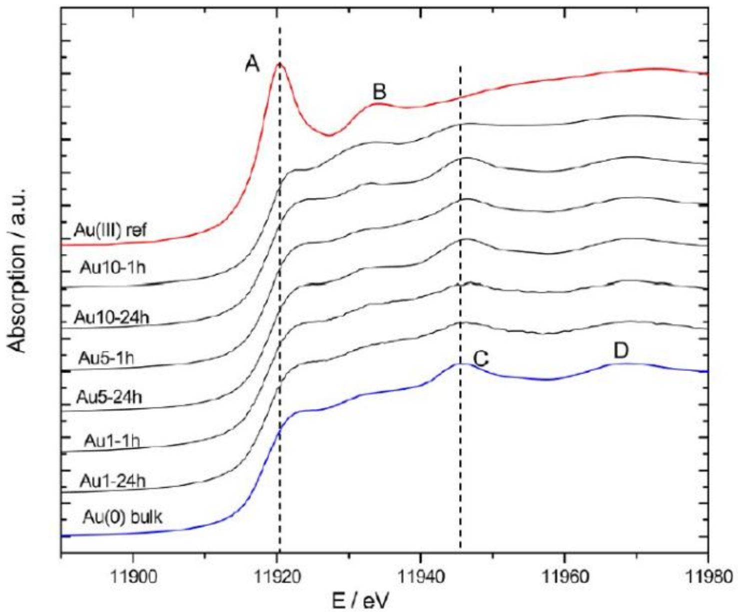


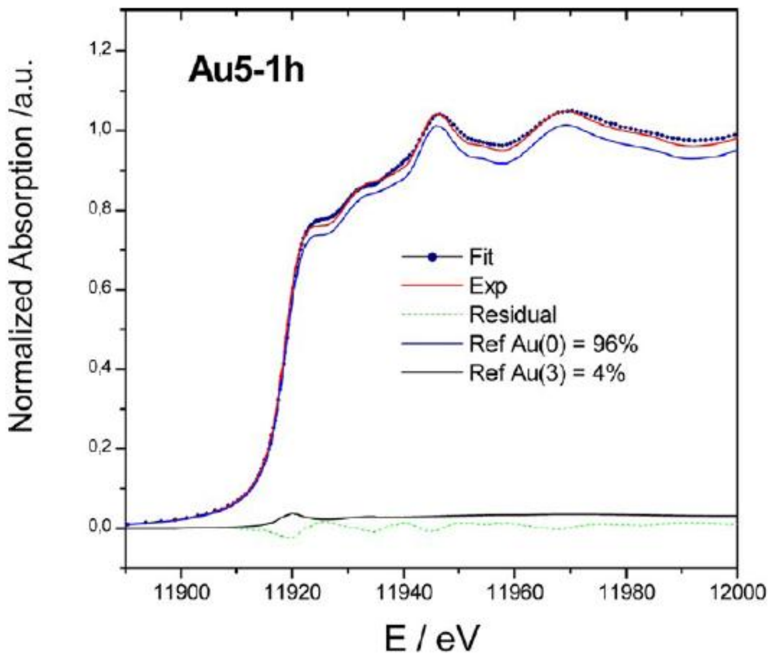


| sample | Norm(E), 20–100 eV wt % Au(0) | wt % Au(III) |
|---|---|---|
| **$Au_{1-1}h$** | 94.5 | 5.5 |
| **$Au_{5-1}h$** | 96.7 | 3.3 |
| **$Au_{10-1}h$** | 67.1 | 32.9 |
| **$Au_{1-24}h$** | 93.1 | 6.9 |
| **$Au_{5-24}h$** | 99.2 | 0.8 |
| **$Au_{10-24}h$** | 96.8 | 3.2 |
| **$Au_{10-1}h$ (recycled)** | 90.9 | 9.1 |

S. Fazzini et al., J. Phys. C **116** 25434 (2012)

# Nanomaterials: size determination

## Local order of nanostructured Pt

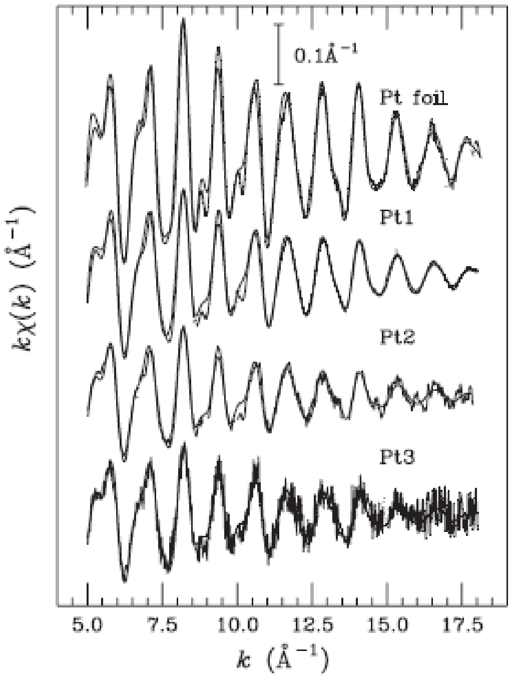


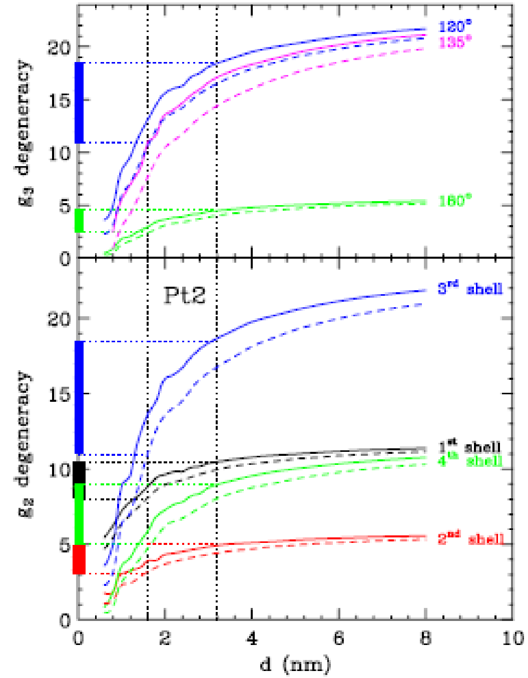


| Shell | Pt foil | | | | Pt1 | | | | Pt2 | | | | Pt3 | | | |
|---|---|---|---|---|---|---|---|---|---|---|---|---|---|---|---|---|
| | $R$ | $\sigma^2$ | $\beta$ | $N$ | $R$ | $\sigma^2$ | $\beta$ | $N$ | $R$ | $\sigma^2$ | $\beta$ | $N$ | $R$ | $\sigma^2$ | $\beta$ | $N$ |
| I | 2.766(2) | 4.9(1) | 0.00(5) | $12.0_f$ | 2.761(2) | 5.8(1) | 0.06(5) | 11.3(5) | 2.768(5) | 6.9(5) | 0.2(1) | 9.6(8) | 2.77(1) | 7(1) | 0.2(2) | 9.3(1.0) |
| II | 3.909(5) | 7.4(8) | 0.00(5) | $6.0_f$ | 3.903(5) | 8.3(8) | 0.00(5) | 5.2(5) | 3.91(1) | 8(2) | 0.1(2) | 4.5(8) | 3.91(2) | 9(4) | 0.1(5) | 4.4(1.5) |
| III[a] | 4.790(4) | 7(3) | $0.0_f$ | $24.0_f$ | 4.782(4) | 8(4) | $0.0_f$ | 21(2) | 4.79(1) | 8(5) | $0.0_f$ | 16(3) | 4.79(2) | 8(7) | $0.0_f$ | 15(6) |
| IV[a] | 5.528(4) | 9(3) | $0.0_f$ | $12.0_f$ | 5.518(4) | 10(4) | $0.0_f$ | 11(1) | 5.53(1) | 10(5) | $0.0_f$ | 8(2) | 5.52(2) | 10(7) | $0.0_f$ | 8(3) |

A. Witkowska et al., Phys. Rev. B **76** 104110 (2007)

# $Cu^{2+}$-loaded Cu hexacyanoferrate

M. Giorgetti et al., PCCP **14**, 5527 (2012),
M. Giorgetti et al., J. Phys.: Conf. Series 430, 012049 (2013)

$A_xM_y[Fe(CN)_6]\cdot zH_2O$

"soluble"* structure (F-43m)

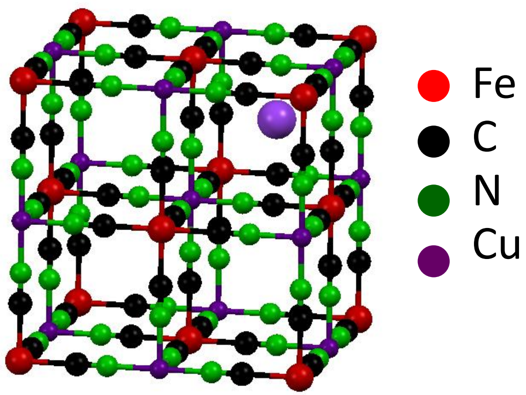


- a ~ 10.2 Å
- alkaly metals occupy intertitial 8c positions
- **-CN-Cu-NC-Fe-CN-** linear chains
- Fe and Cu in octahedral sites

  6 x Fe-CN-Cu
  6 x Cu-NC-Fe

"insoluble" * structure (Pm-3m)

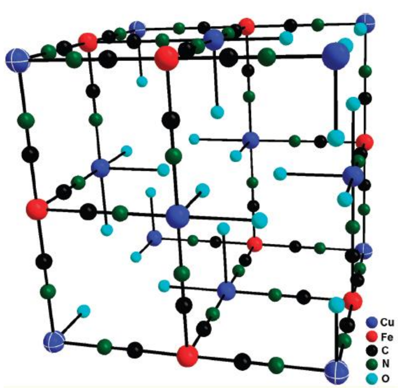


- Model with [**Fe**$(CN)_6]^{3-}$ ion vacancies

6 x Fe-CN-Cu
4.5 x Cu-NC-Fe
1.5 x Cu-O

# $Cu^{2+}$-loaded Cu hexacyanoferrate: interest

## Applications

- Electrochromism
- Electrocatalysis
- Ionic and electronic conductivity
- Charge storage
- Photo-induced magnetisation
- Electro-catalytic oxidation of alcohols in alkaline medium

## Aim of the study

- Relationship between structure and properties
- **Amount of vacancies linked to the ability of H storage**

# Data analysis strategy

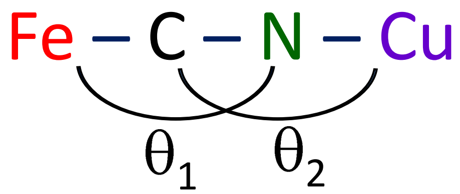


Linear chains between Cu and Fe gives rise to a
*superfocusing effect* and therefore to a *large EXAFS signal*

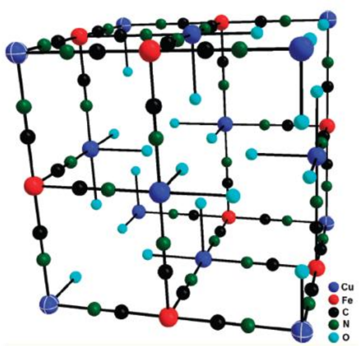


→ Information on the amount of the vacancies

| Signals for the Cu K-edge (CN) | |
|---|---|
| Two body | $\gamma_1^{(2)}$ Cu-N; (4.5) |
| | $\gamma_2^{(2)}$ Cu-O; (1.5) |
| | $\gamma_3^{(2)}$ Cu-K; (*) |
| Three body | $\eta_1^{(3)}$ Cu-N-C; (4.5) |
| Four body | $\eta_1^{(4)}$ Cu-N-C-Fe; (4.5) |

# Copper Hexacyanoferrate: Fe – C – N – Cu

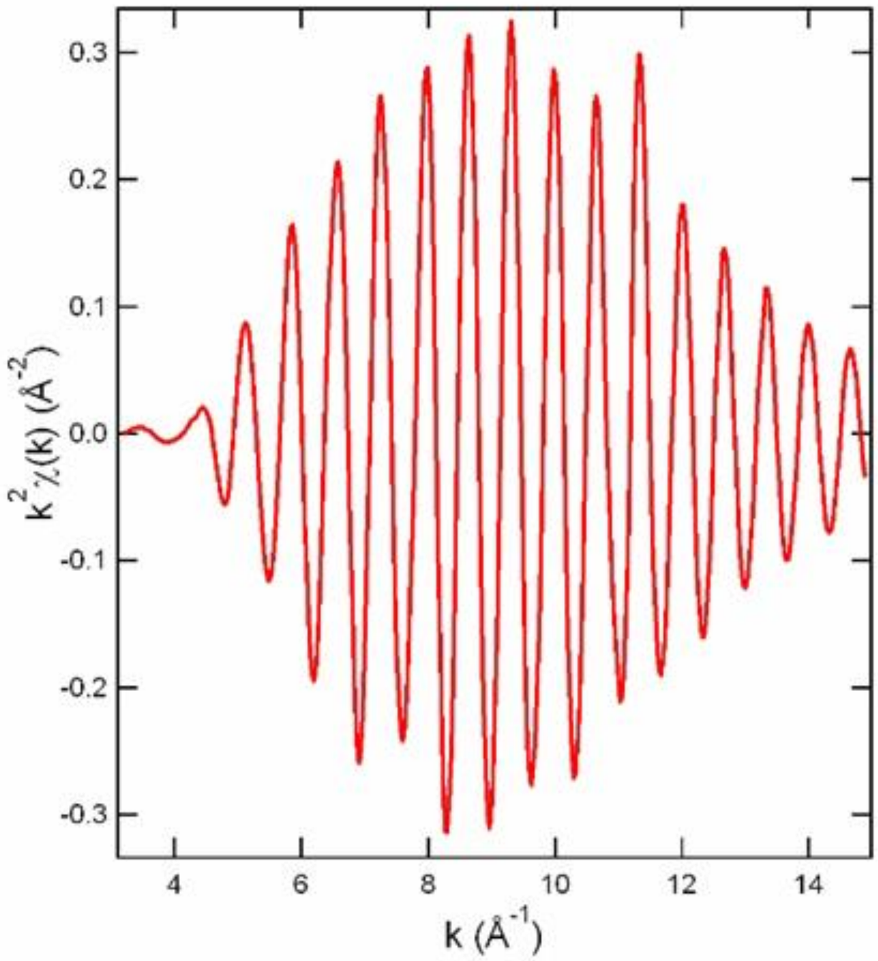


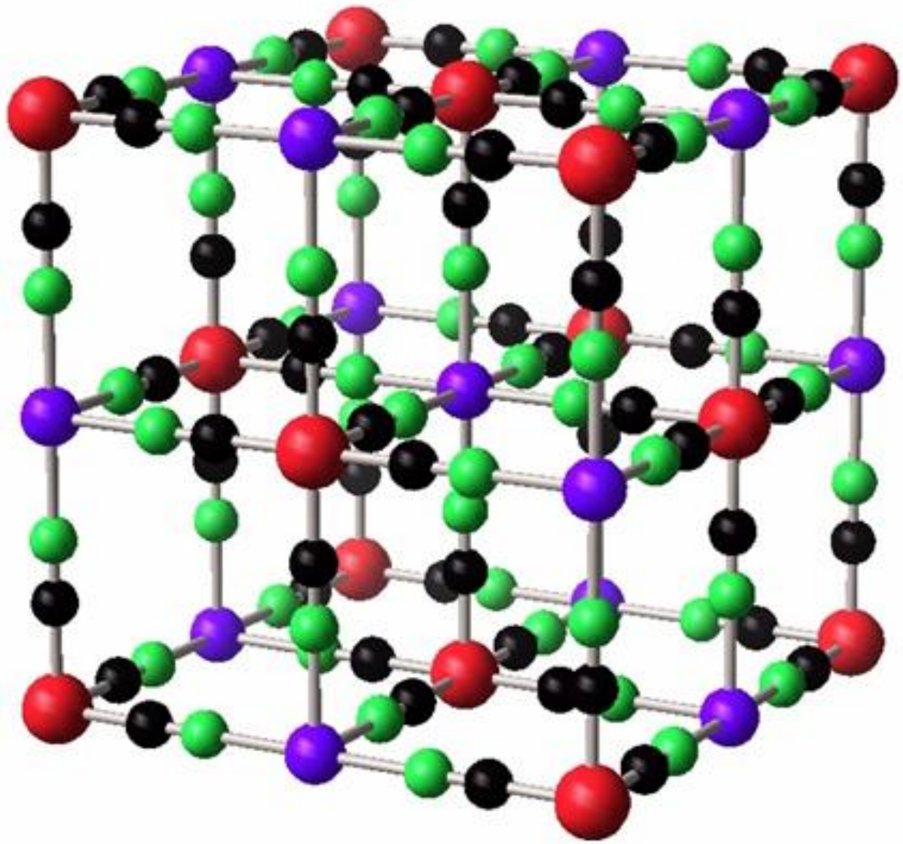

## Copper Hexacyanoferrate: Fe – C – N – Cu

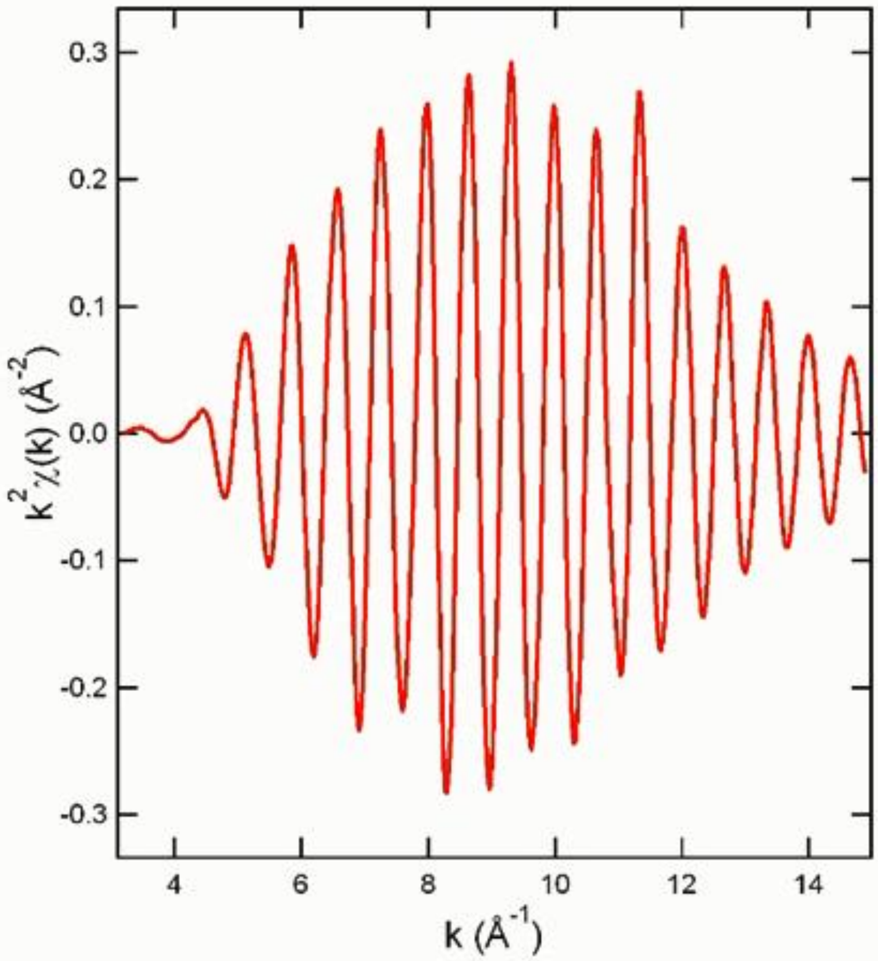


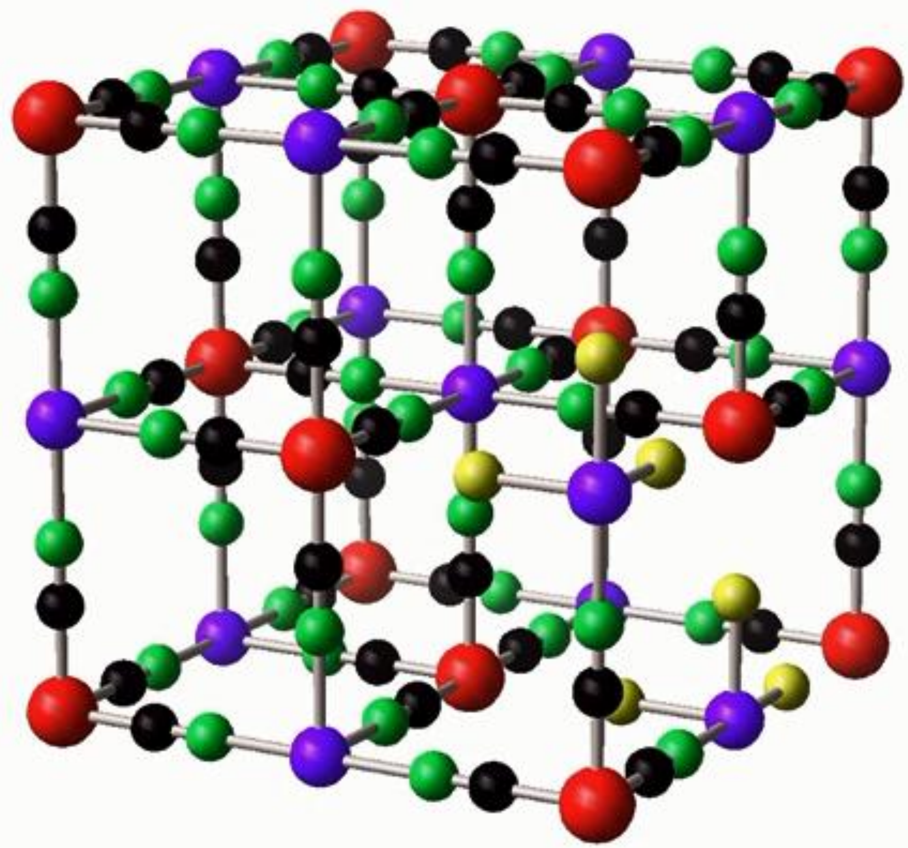

## Copper Hexacyanoferrate: Fe – C – N – Cu

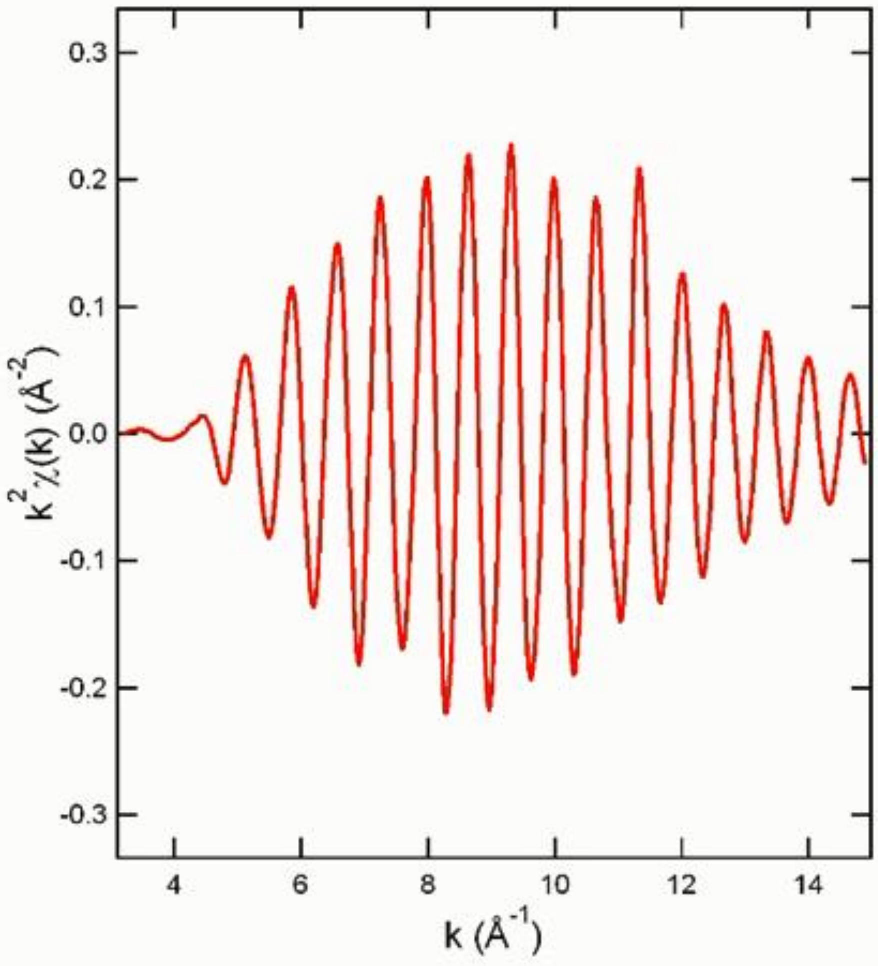


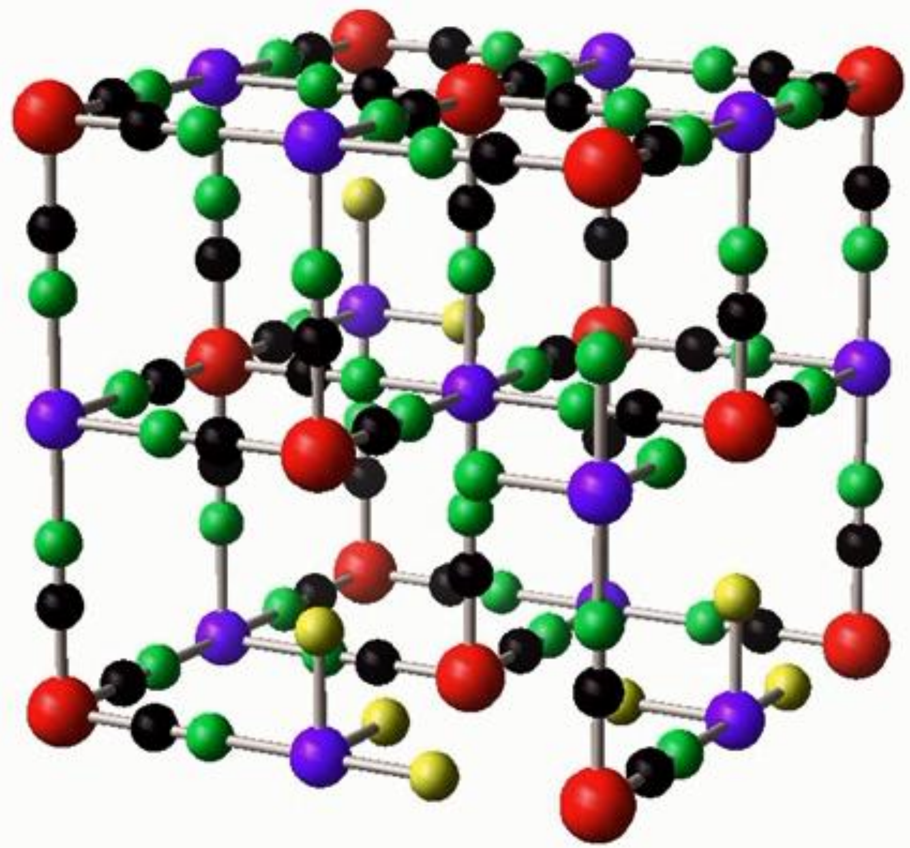

## Copper Hexacyanoferrate: Fe – C – N – Cu

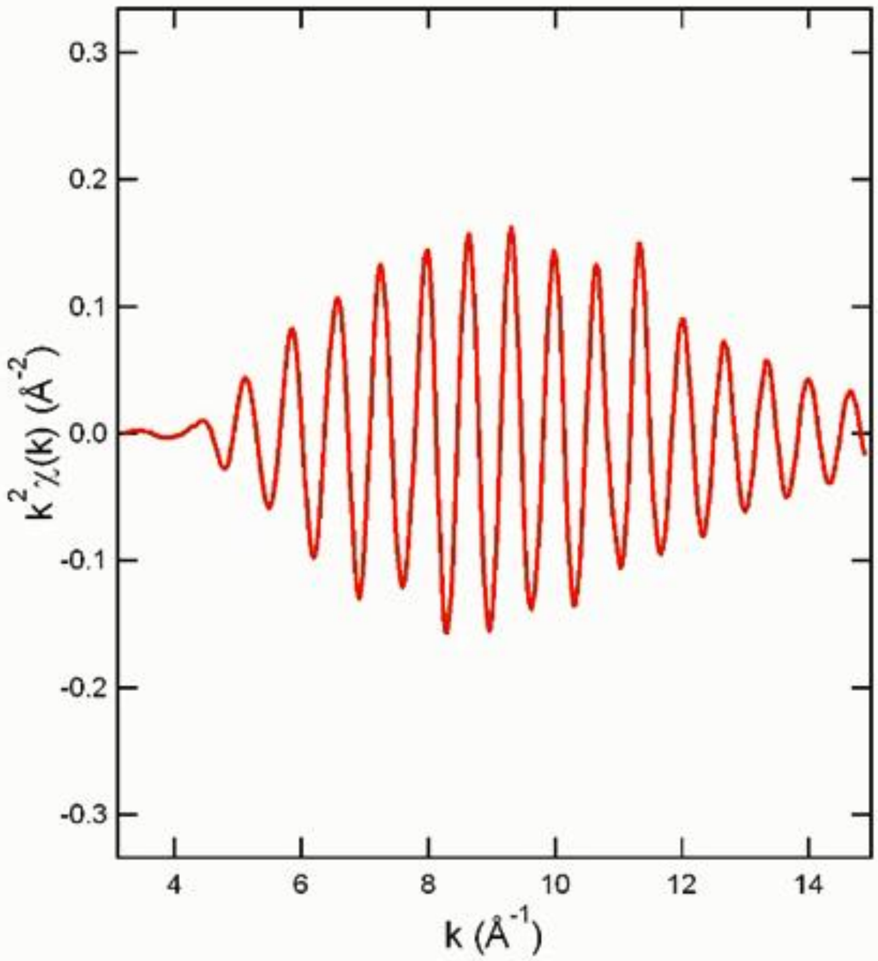


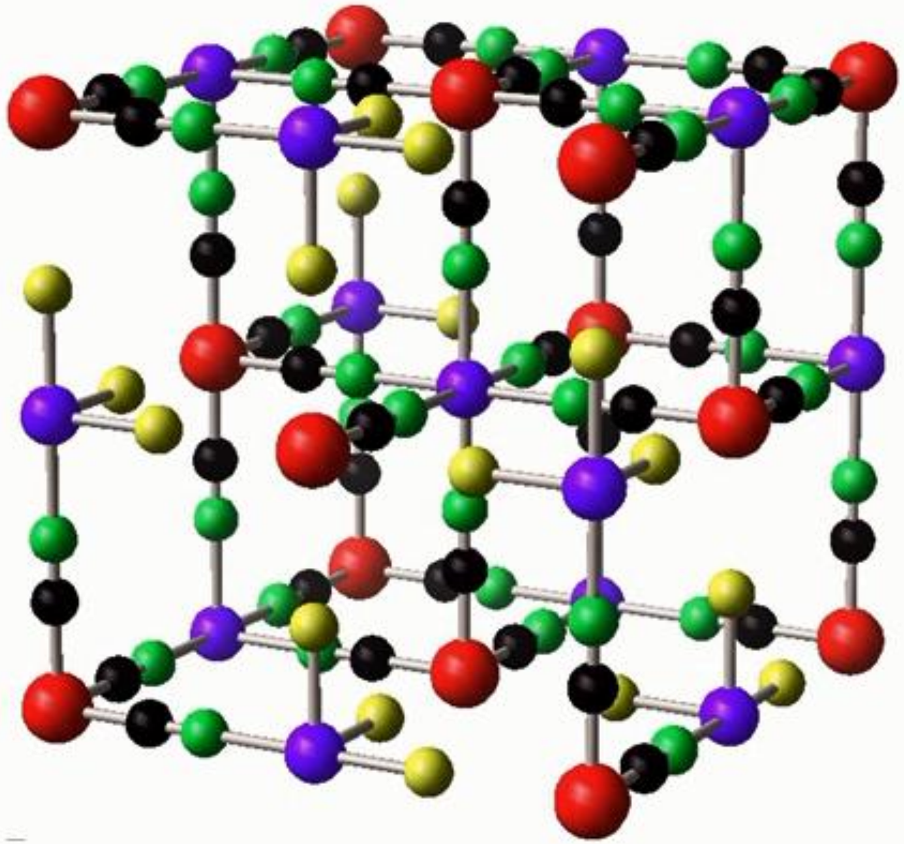

## Copper Hexacyanoferrate: Fe – C – N – Cu

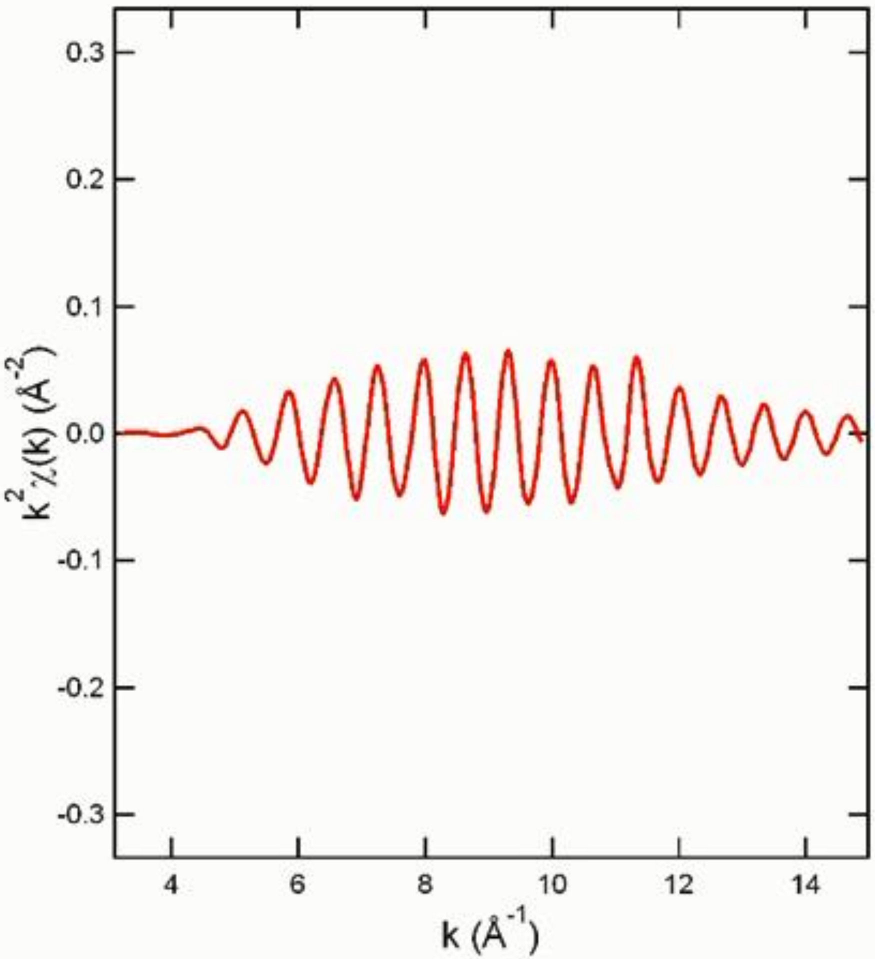


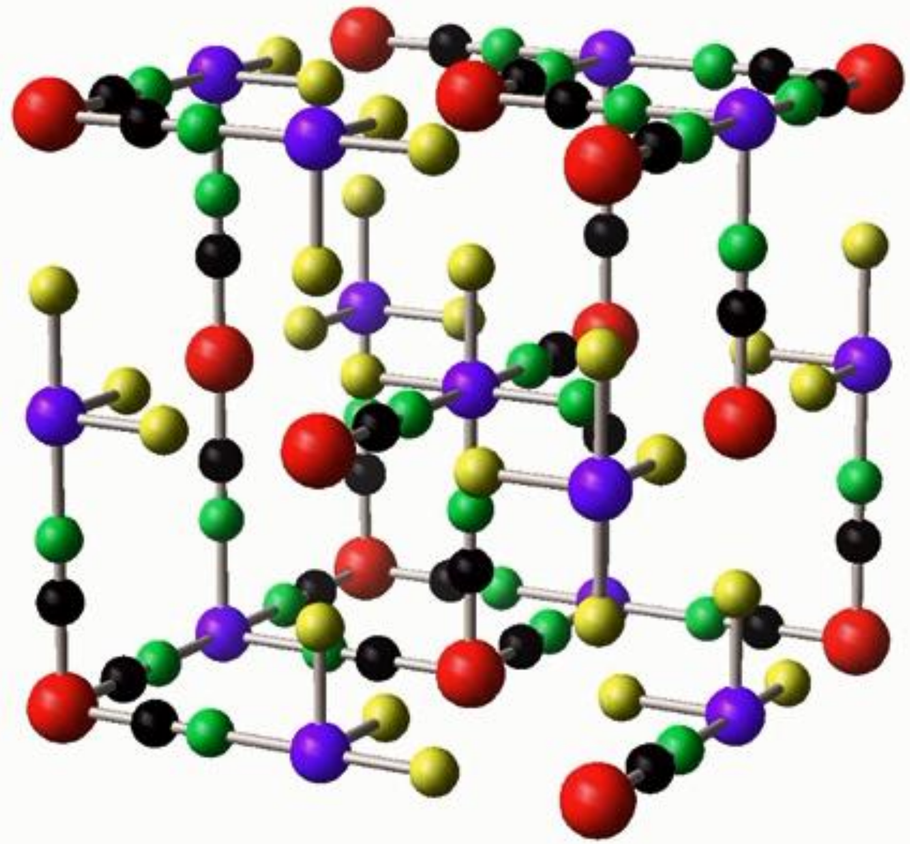

# Fitting results

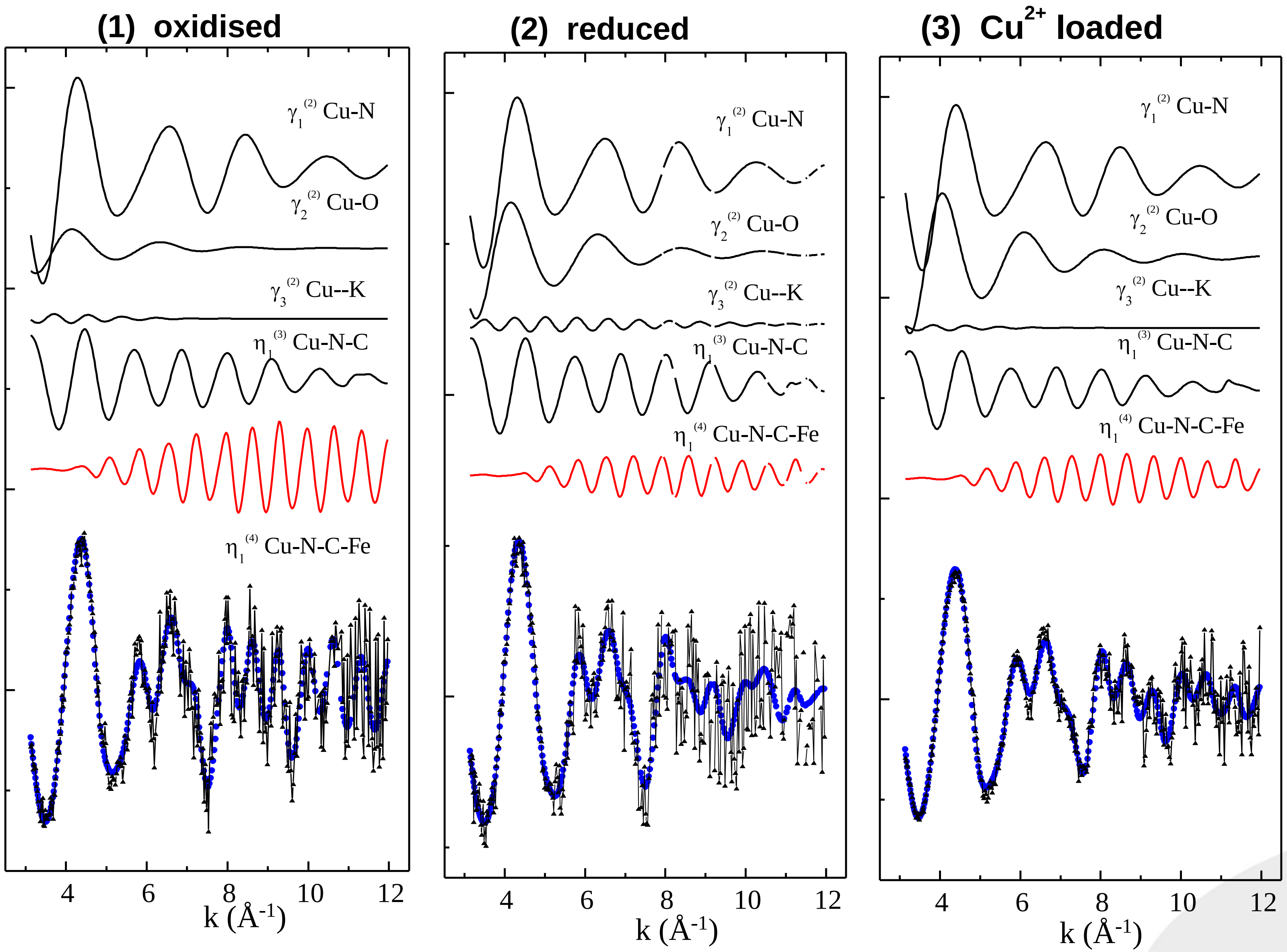

# Magnetite biomineralization in bacteria - 1

M. L. Fdez Gubieda et al., ACS Nano **7** 3297 (2013)

- Many organisms (magnetotactic bacteria) produces magnetic nanoparticles

- Magnetospirillum gryphiswaldense produces magnetite nanoparticles surrounded by a lipidic membrane (magnetosomes)

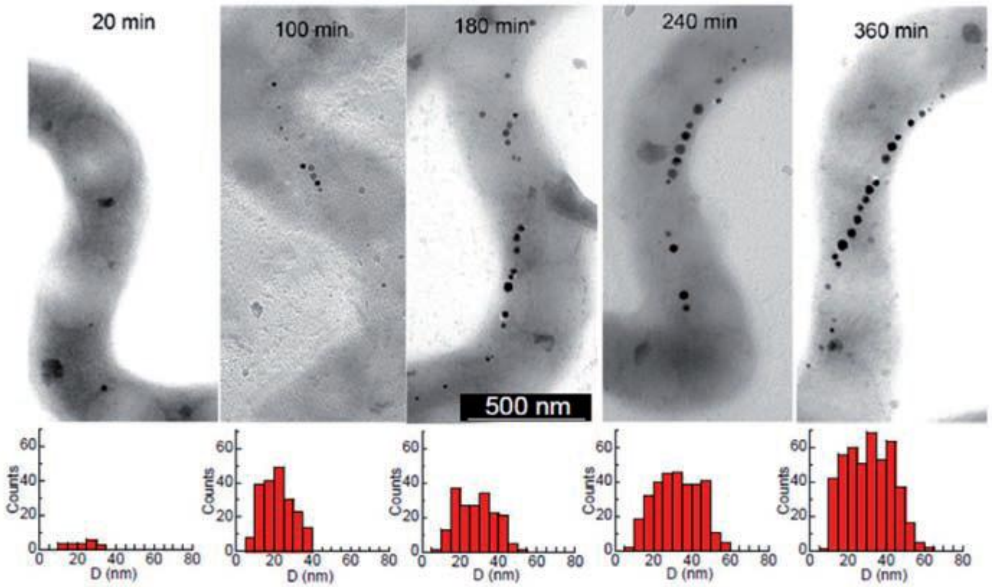


- Chaines used as compass needles to orient in the geomagnetic field
- Good biocompatibility and therefore interesting in biomedical applications
- Understanding of the biomineralization process to design new materials

# Magnetite biomineralization in bacteria - 2

XANES

- To identify the oxidation state and local geometry of the absorbing atom
- To identify and quantify the different Fe phases
- 2 eV shift towards lower energies
- LC of ferrihydrite ($Fe^{3+}$) and magnetite ($Fe^{3+}$ and $Fe^{2+}$)
- ferrihydrite constant and then in the end of the biomineralization process undetectable

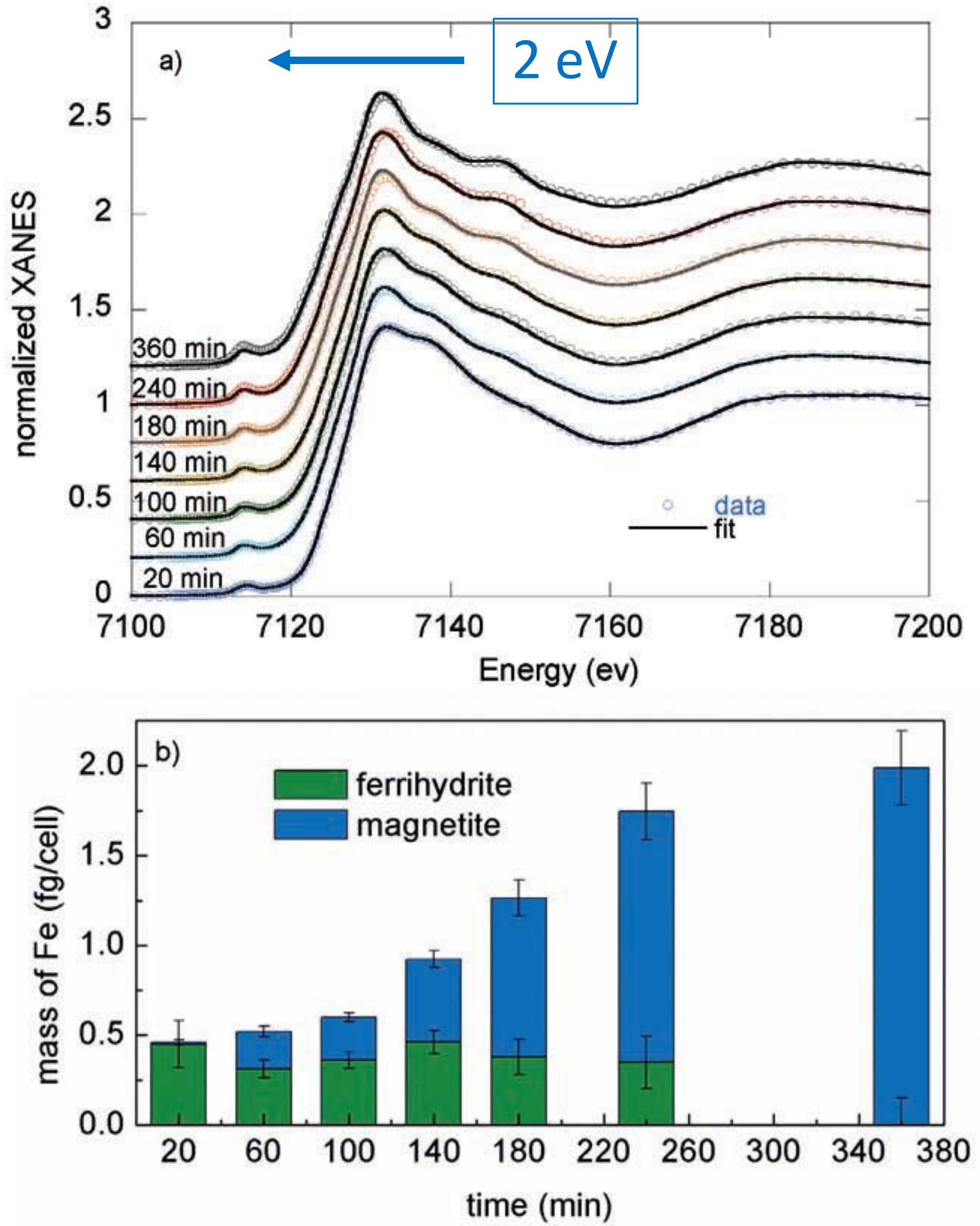

Elettra
Sincrotrone
Trieste

Thank you!

Elettra
Sincrotrone
Trieste

www.elettra.eu